Computational and Theoretical Chemistry 1072 (2015) 43–51

Contents lists available at ScienceDirect

Computational and Theoretical Chemistry

journal homepage: www.elsevier.com/locate/comptc

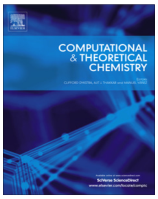

Lithium migration at low concentration in TiO_2 polymorphs

Corinne Arrouvel [a,b,c,*], Thiago C. Peixoto [b,d], Mario E.G. Valerio [b], Stephen C. Parker [a]

[a] University of Bath, Department of Chemistry, Bath BA2 7AY, UK
[b] Universidade Federal de Sergipe, Departamento de Física, São Cristóvão, Sergipe 49100-000, Brazil
[c] Universidade Federal de São Carlos, DFQM, Sorocaba, SP 18052-780, Brazil
[d] Universidade Estadual Paulista, Instituto de Física Teórica, São Paulo, SP 01140-070, Brazil

ARTICLE INFO

Article history:
Received 22 July 2015
Received in revised form 2 September 2015
Accepted 2 September 2015
Available online 7 September 2015

Keywords:
Lithium-ion batteries
Anode
Atomistic simulations
3D pathways
TiO_2-B
Anatase

ABSTRACT

We report an atomistic simulation study at low concentration of lithium in scanning all the possible pathways for Li migration in TiO_2 polymorphs. We are particularly interested in showing the effects of the structural properties on the intercalation energies and on the energy barriers for ion diffusion. The most favourable directions for Li^+ transport are highlighted and we observe an anisotropic diffusion in rutile, brookite and TiO_2-B whereas the diffusion is isotropic in the case of anatase. The lowest energy barrier is calculated in rutile but it is not a key factor to determine the efficiency of Li-battery materials. Intercalation energies of stable and transition states are however important data to take into account as well as the Li pathway in order to evaluate the potentiality of each polymorph for Li migration.

1. Introduction

The migration of extrinsic and intrinsic defects plays a key role in many industrial applications such as lithium-ion batteries and fuel cells. However, understanding the mechanism of the intercalation and diffusion at the atomic scale is often not well understood.

Recent reviews and theoretical work [1–6] have been devoted to anode and cathode electrodes. Titanium oxides are very promising anode materials and particularly the TiO_2-B phase. TiO_2-B shows a higher capacity [7–9] (up to 338 mA h/g on nanotubes [8] and more recently up to 360 mA h/g on nanoribbons [10]) than the other polymorphs. This phase is less dense than rutile, anatase and brookite phases (respectively 3.73–3.75 g/cm^3 [11,12], 4.26 g/cm^3 [13], 3.92 g/cm^3 [13], 4.12 g/cm^3 [14]) which can explain its efficiency for Li-batteries. Also, there are numerous theoretical and experimental studies on the intercalation of lithium in rutile and anatase [15–33], there is an increasing number of studies on TiO_2-B [3–7,23,32,34–38], few studies on other phases of titania [39–43], rarer on brookite [6,44–48] and scarce on amorphous TiO_2 [49,50]. Like the rutile, the brookite phase has shown no attractiveness for Li-battery unless we reach the nanoparticle size. Only small nanoparticles allow to intercalate a decent quantity of lithium (up to 0.95 Li/Ti in brookite [44], up to 0.85 Li/Ti in rutile [51]) and phase transformations are frequently observed in the case of anatase and rutile [51–53]. The migration of Li is another important point to understand. The ionic diffusion coefficients are difficult to obtain experimentally and a wide range of values has been reported due to the fact that the diffusion can be calculated microscopically or macroscopically. For example, on the anatase phase, various values on the Li diffusion coefficient can be found in the literature, from 10^{-12} to 10^{-17} cm^2/s [26,54]. Other phenomena influence the diffusion coefficient such as the temperature (the coefficient increases as the temperature increases) and the phase transformation (anatase transforms reversibly to an Li-titanate phase around Li/Ti ~ 0.5 and the coefficient decreases [26,30]). The highest Li diffusion coefficient has been experimentally measured for the rutile phase [55] (anisotropic diffusion of 2.7×10^{-3} cm^2/s along the *c* direction with an activation energy of 0.3 eV) at the meantime, the main obstacle is to intercalate Li in large particle sizes [51]. The activation energy in the case of TiO_2-B is about 0.48 eV [56].

We use empirical methods to give new insights on the Li migration through a systematic study. The specific purpose of this work is to detail the diffusion pathways, intercalation sites and to explain the potentiality of Li-battery materials through their energetic and structural properties.

---

* Corresponding author at: Universidade Federal de São Carlos, DFQM, Sorocaba, SP 18052-780, Brazil.
E-mail address: corinne@ufscar.br (C. Arrouvel).

http://dx.doi.org/10.1016/j.comptc.2015.09.002

2. Methods

The atomistic simulations are undertaken using METADISE [57] (Minimum Energy Techniques Applied to Dislocation, Interface, and Surface Energies) and GULP [58,59] (General Utility Lattice Program). METADISE has been mainly used to scan the different pathways in TiO_2 polymorphs and GULP is used to refine the punctual defect calculations.

2.1. Interatomic potential methods

The simulations with METADISE and GULP are based on a Born model of solid assuming that the ions interact via long-range electrostatic forces (Coulombic interactions) and short-range forces including both the repulsions and the van der Waals attractions between neighbouring electron charge clouds [60]. In this study, different potentials have been tested and we have opted for interatomic potentials from Kerisit et al. [6] with a core–shell model which was derived from Matsui and Akoagi (MA) potentials [61] for TiO_2. $LiTiO_2$ potentials have been further tested and compared to previous DFT calculations on TiO_2-B [3,4] and experimental data [36].

The potentials follow the relation:

$$V_{r_{ij}} = \sum \frac{q_i q_j}{r_{ij}} + A_{ij} \exp(-r_{ij}/\rho_{ij}) - \frac{C_{ij}}{r_{ij}^6}$$

With r_{ij} the separation between the ions i and j; q_i and q_j the charges of each ion acting in the Coulombic term; and A_{ij}, ρ_{ij}, C_{ij} the ion–ion parameters in the Buckingham relation.

2.2. Scan of Li pathways

One of the strengths of using interatomic potential models is that the total energy of the system can be evaluated rapidly. Thus we are able to exploit this by performing a simple scan of the total interaction energy as a function of the lithium position. This is achieved by simply adjusting the position of the lithium ion in steps of 0.1 Å within the unit cell, and then calculating the energy. As we use the shell model, after each update of the lithium position we allow the shells to relax and hence this mimics to a limited extent electronic relaxation and provides an approximate representation of the polarisation of the crystal as the lithium is moved through the lattice. The energies are calculated using the METADISE [57] code and the energy profile and the isosurfaces are plotted using VESTA [62].

2.3. Defect calculations

GULP uses the Mott–Littleton approach [63], which is also a two-regions approach. The region I is around the defect (Li^+ intercalation in our case) and is allowed to fully relax. The region II surrounding the region I is fixed and represents the rest of the crystal involving quasi-continuum methods. The sizes of the two regions are 14 Å (region I) and 22 Å (region II).

We note that the defect calculation is referred to the intercalation of the Li^+ in the gas phase, therefore this value can be directly compared to the voltage, or intercalation of Li metal. However, the relative energies between defect calculations should follow the same trend at low concentration if we consider that the energetic process to transform Li metal in Li gas, to oxidise Li into Li^+ and to reduce the Ti network is the same for all the polymorphs.

3. Results

3.1. Bulk crystal structures of TiO_2 polymorphs

The bulk crystal structures of rutile [64], anatase [65], brookite [66] and TiO_2-B [11] obtained from X-ray data are summarised in Table 1. Most of TiO_2 polymorphs have Ti species with a coordination number of 6 and O species with a coordination of 3. The exception is for TiO_2-B which has O ions with different coordination numbers of 2, 3 and 4.

The bulk crystal structure of the polymorphs has already been calculated and well detailed by Kerisit et al. [6]. To better understand the Li intercalation and diffusion, we summarise few key energetic and structural characteristics in Table 2. The stability order using minimisation techniques with Kerisit et al.'s potential is as follows:

$$\text{Rutile} > \text{Brookite} > \text{Anatase} > TiO_2\text{-B}$$

The density and the average of Ti–O distances follow the same order, the rutile phase being the densest and getting the shortest average Ti–O distances. The TiO_2-B phase is interesting for Li-ion batteries, being the less dense of those polymorphs and having a higher experimental capacity. The range of distances is wider; this phase gets the shortest and the longest Ti–O distances. The shortest Ti–O distances are linked to the 2-fold oxygen (about 1.84 Å) and a relatively wide infinite channel is between the 2-fold oxygens. Another channel is visible along the *c* direction of TiO_2-B. In the case of the rutile phase, a channel can be observed along the *c* direction but due to the denser structure, the channel is thinner.

3.2. Pathways for Li migration

The energy profiles for each polymorph obtained with METADISE are shown in Fig. 1 and the most stable channels for the Li diffusion are represented. The centre of the channels, where the

Table 1
Structural characteristics of experimental TiO_2 polymorphs.

	Rutile [64]	Anatase [65]	Brookite [66]	TiO_2-B [11]
Space group (number)	$P4_2/mnm$ (136)	I 4_1/amd (141)	Pbca (61)	C2/m (12)
Crystal system	Tetragonal	Tetragonal	Orthorhombic	Monoclinic
a (Å)	4.60	3.78	9.18	12.18
b (Å)	4.60	3.78	5.45	3.74
c (Å)	2.96	9.51	5.14	6.52
Cell volume (Å^3)	62.61	136.26	257.38	284.22
Density (g/cm^3)	4.24	3.89	4.12	3.73
Number of TiO_2 units, Z	2	4	8	8
Ti–O distance range	1.97 ∗ 2	1.98 ∗ 2	1.99	1.81–2.26
	1.96 ∗ 4	1.93 ∗ 4	1.87	
			1.99	
			1.92	
			1.94	
			2.04	